

Enhancing Brain Age Estimation with a Multimodal 3D CNN Approach Combining Structural MRI and AI-Synthesized Cerebral Blood Volume Data

Authors

Jordan Jomsky

jordan.jomsky@columbia.edu

Department of Data Science, Columbia University, New York, NY, USA

Zongyu Li

zl3372@columbia.edu

Department of Biomedical Engineering, Columbia University, New York, NY, USA

Yiren Zhang

yiren.zhang@columbia.edu

Department of Biomedical Engineering, Columbia University, New York, NY, USA

Tal Nuriel

tn2283@columbia.edu

Taub Institute for Research on Alzheimer's Disease and the Aging Brain, Columbia University, New York, NY, USA

Jia Guo

jg3400@columbia.edu

Mortimer B. Zuckerman Mind Brain Behavior Institute, Columbia University, New York, NY, USA

Data Availability Statement

All data was obtained from publicly available studies.

Funding Availability Statement

This work was supported by a grant from the Simons Foundation (811245, S. S.).

Enhancing Brain Age Estimation with a Multimodal 3D CNN Approach Combining Structural MRI and AI-Synthesized Cerebral Blood Volume Data

Jordan Jomsky¹, Zongyu Li², Yiren Zhang², Tal Nuriel³, Jia Guo^{4*}

¹ Department of Data Science, Columbia University, New York, NY, USA

² Department of Biomedical Engineering, Columbia University, New York, NY, USA

³ Taub Institute for Research on Alzheimer’s Disease and the Aging Brain, Columbia University, New York, NY, USA

⁴ Mortimer B. Zuckerman Mind Brain Behavior Institute, Columbia University, New York, NY, USA

Abstract. The increasing global aging population necessitates improved methods to assess brain aging and its related neurodegenerative changes. Brain Age Gap Estimation (BrainAGE) offers a neuroimaging biomarker for understanding these changes by predicting brain age from MRI scans. Current approaches primarily use T1-weighted magnetic resonance imaging (T1w MRI) data, capturing only structural brain information. To address this limitation, AI-generated Cerebral Blood Volume (AICBV) data, synthesized from non-contrast MRI scans, offers functional insights by revealing subtle blood-tissue contrasts otherwise undetectable in standard imaging. We integrated AICBV with T1w MRI to predict brain age, combining both structural and functional metrics. We developed a deep learning model using a VGG-based architecture for both modalities and combined their predictions using linear regression. Our model achieved a mean absolute error (MAE) of 3.95 years and an R^2 of 0.943 on the test set ($n = 288$), outperforming existing models trained on similar data. We have further created gradient-based class activation maps (Grad-CAM) to visualize the regions of the brain that most influenced the model’s predictions, providing interpretable insights into the structural and functional contributors to brain aging.

Keywords

MRI, brain age, CBV, deep learning

Key Points

- Integrating AI-synthesized cerebral blood volume (AICBV) data with T1w MRI improves brain age estimation accuracy.
- Performance surpasses T1w-only models, achieving a mean absolute error of 3.95 years on a large, diverse dataset.
- Further analyses reveal the concordance of structural and functional vulnerable regions influencing brain aging predictions.

1 Introduction

Aging is one of the only diseases that affects everyone. With an aging global population, there is an even greater need to increase our understanding of brain aging, in order to develop interventions to support cognitive health and prevent age-related neurological disorders. While aging impacts every organ of the body, its effects on the brain are particularly unique with both structural and functional changes occurring in the brain with age [17, 11].

Brain Age Gap Estimation (BrainAGE) has emerged as a promising research avenue for developing a neuroimaging-based biomarker of brain aging. Current BrainAGE research primarily utilizes T1-weighted magnetic resonance imaging (T1w MRI) scans due to their cost-effectiveness, non-invasive nature, and widespread clinical use. Feng et al. demonstrated the effectiveness of the T1w MRI modality as input data for a VGG-based model, achieving a mean absolute error of 4.06 and R^2 of 0.941 [6]. However, T1w MRI captures only structural information, lacking insight into brain function. Combining structural and functional imaging modalities to determine BrainAGE would offer a more comprehensive evaluation and understanding of brain aging.

* Corresponding author: jg3400@columbia.edu

There are numerous existing functional neuroimaging modalities; however, each of these modalities possesses unique limitations that prevent their use for BrainAGE. Fluorodeoxyglucose positron emission tomography (FDG PET) is an excellent technique for measuring regional glucose uptake in the brain; however, its higher cost and use of radiation limit its widespread application [8]. Furthermore, while functional magnetic resonance imaging (fMRI), particularly blood-oxygen-level-dependent (BOLD) imaging, is non-invasive, its limited spatial resolution makes it challenging to study small brain structures quantitatively [9].

Perfusion MRI techniques, such as cerebral blood flow (CBF) and cerebral blood volume (CBV) imaging, provide higher-resolution information about brain function [2, 20]. Among these, steady-state CBV mapping with contrast enhancement stands out as the only functional neuroimaging approach capable of achieving spatial resolution comparable to T1w MRI scans [15, 18]. This makes CBV imaging a valuable complement to conventional MRI for detecting and characterizing brain functional changes. However, CBV requires injection of a contrast agent such as gadolinium-based contrast agents (GBCAs), which contains the highly toxic element gadolinium that can have potentially lethal side effects including nephrogenic systemic fibrosis [10]. Furthermore, large-scale, resolution-matched functional perfusion datasets, such as steady-state CBV imaging, are not readily available, limiting the ability to fully exploit functional imaging to complement structural data.

This highlights the critical need for complementary datasets in BrainAGE research to capture the complex interplay between structural atrophy and functional changes, enabling deeper insights into aging patterns and the development of robust biomarkers for brain health. To address this limitation, we have utilized AI-derived Cerebral Blood Volume (AICBV), an innovative approach that extracts functional information from T1w MRI scans. This advancement offers the potential to create a more comprehensive, novel BrainAGE model that integrates both structural T1w MRI and functional AICBV data, potentially improving the accuracy and clinical utility of brain age predictions.

Originally generated by our group, AICBV builds upon the idea that non-contrast MRI scans inherently contain subtle blood-tissue contrasts that, while challenging to detect with traditional methods, can be revealed using deep learning techniques [12]. The approach leverages machine learning models to extract GBCA-equivalent information without the need for invasive contrast agents, identifying subtle patterns in voxel intensities that distinguish blood vessels from surrounding tissues—patterns that are theoretically present but not visually apparent due to the intrinsic T1w relaxation time differences among blood, gray matter, and white matter. The method has been applied to both in-house datasets and publicly available ones, such as ADNI, showing its potential to localize functional abnormalities and improve diagnostic accuracy in neurodegenerative diseases. By integrating AICBV-derived functional information into the BrainAGE model, we aim to improve the clinical utility of MRI for assessing brain health, offering a non-invasive alternative to contrast agents and broadening the scope of neurological research by enabling retrospective analyses of existing MRI data.

Further novelty in this approach lies in the combination of structural and functional brain scan data used in tandem to train these models, especially given full 3D context. Typical deep learning models that perform BrainAGE derivation leverage models and architectures for image processing and classification built for 2D images. However, even with fine-tuned, state-of-the-art 2D models, critical information can be lost without accounting for the three-dimensional complexity of brain structures. To overcome this, we employ 3D convolutional and batch norm layers in our architecture that preserve spatial relationships within the brain, capturing subtle anatomical and functional variations from both data modalities. This 3D approach allows for deeper insights into how structural and functional changes interact throughout the aging process. By integrating AICBV with T1w MRI, our model aims to achieve more precise brain age predictions that uniquely incorporate 3D structural and functional information.

2 Methods

This study did not require ethical approval as it relied on publicly available anonymized MRI scans that were originally collected as part of studies already approved by requisite standards.

2.1 Data Information

In this study, we leveraged neuroimaging and clinical data from 13 publicly available datasets: Alzheimer’s Disease Neuroimaging Initiative (ADNI), Brain Genomics Superstruct Project (BGSP), Neuroimaging in Frontotemporal Dementia (NIFD), Stress and Limbic Modeling (SLIM), Dallas Lifespan Brain Study (dlbs), Southwest Advanced Life-course Development (SALD), Australian Imaging, Biomarkers & Lifestyle Study of Aging (AIBL), Consortium for Reliability and Reproducibility (CoRR), SchizConnect, Information eXtraction from Images (IXI), Open Access Series of Imaging Studies (OAS1 and OAS2), and the Parkinson’s Progression Markers Initiative (PPMI). The data includes 2,851 T1w MRI images. These images follow the MNI-152 coordinate system with an affine transformation. This is the most popular standardized protocol for these images, maximizing the generalizability and applicability of the results. The diverse data sources in this study enhance the transferability of our findings to future studies and clinical applications.

Figure 1 showcases the distribution of age of each of the patients across the dataset, each study, and the data split used to train and validate the model. This plot highlights the variability in age ranges across the studies used to train our model.

2.2 AICBV Model

To enhance our model’s understanding of the functional aspect of the brain, we utilized a 3D patch-based hybrid CNN-Mamba model to generate the AICBV from each MRI scan. The Mamba model merges the advantages of Transformers and RNNs, enabling efficient parallel training and linear-time sequence labeling during inference, thus reducing computational costs and processing high-resolution images with fewer parameters and less memory usage. Specifically, it features a 3D Visual State Space (VSS3D) block that resembles a traditional Transformer block but replaces self-attention with a 3D Selective Scan (SS3D) block inspired by the Hilbert scanning method, capturing intricate spatial relationships in 3D volumes by processing data along various paths and enhancing tasks like segmentation and prediction. The overall architecture includes a 3D CNN encoder and decoder with skip connections and a Vision Transformer module in between, with key features including a bottleneck layer containing nine VSS3D blocks that improve data encoding through selective scanning and parallel processing, ultimately reconstructing the image to its original dimensions with a one-channel output [12].

2.3 Model Structure

A VGG8 architecture was implemented in this project in PyTorch. Each block consisted of a 3D convolution, 3D batch norm, ReLU activation, and 3D max pooling layer with 5 of these blocks making up the encoder of this model. The number of out channels in each convolution layer was 16, 32, 64, 128, and 256. The next 3 layers consisted of fully connected layers going from the respective flattened size of the encoder output to 512 to 128 to 1 to get the final brain age prediction.

A linear regression model was implemented in R to combine the predictions from each model. Each model’s prediction was combined and used as a feature to predict the actual age of the patient. This combined approach integrates structural and functional age estimates, leveraging the unique strengths of each model. Figure 2 showcases the full model pipeline from data collection to inference as described in this section.

2.4 Model Training Process

The dataset was first stratified based on age. Specifically, the age distribution was divided into deciles using the quantile function, which identified the 10th to the 90th percentiles of the age variable. The resulting quantiles, along with the minimum and maximum age values, were used to define the bin edges, and each scan was accordingly assigned to these age bins. The dataset was partitioned into ten separate stratified partitions based on age bins as well as project origin of the scan. The dataset of 2,851 scans was split in a 8:1:1 ratio into training, validation, and test sets. The validation and test set were selected from the ten partitions with minimal KL divergence compared to the dataset overall to ensure generalizable performance.

To preprocess the scans effectively for a deep learning model, each scan needed to be normalized. Utilizing a modified min-max scaling process, each scan is divided by the average of its top 1% of values, effectively normalizing each scan.

The VGG model for both T1w and AICBV scans was trained for 100 epochs with an early cutoff if the mean absolute error (MAE) did not improve over 10 epochs. An Adam optimizer with a learning rate of 1×10^{-4} and MAE loss were used to train the model with a batch size of 3. All models were trained on the NVIDIA RTX A6000 GPU. After each model completed training, train, validation, and test predictions were extracted from both models. Training and validation predictions from the T1w- and AICBV-trained models were used as input for a linear regression model to predict brain age. Final test predictions were then obtained from this linear regression model.

3 Results

In this section, we present the results of our analyses to evaluate the predictive performance of our models across the various input feature sets, as well as their robustness across the test dataset’s different age and study groups. Additionally, we explore the interpretability of our models by examining the spatial focus of their predictions using gradient-based class activation maps (Grad-CAM).

3.1 Overall Performance

Model	Mean Absolute Error (MAE)	Mean Squared Error (MSE)	R ²	ANOVA p-value
T1w only (T-model)	4.10	29.02	0.936	-
AICBV only (A-model)	4.49	33.34	0.927	-
T1w + AICBV (TA-model)	3.96	26.07	0.943	T vs TA: $< 2.2 \times 10^{-16}$ *
T1w + AICBV + sex (TAS-model)	3.95	25.98	0.943	A vs TA: $< 2.2 \times 10^{-16}$ * TA vs TAS: 0.02 *

Table 1: Performance metrics for models incorporating T1w MRI, AICBV, and sex as features. * denotes statistical significance at $p < 0.05$.

We compared the results on the test data of four linear regression models created from our model architecture: (1) T1w-predicted age only (T-model), (2) AICBV-predicted age only (A-model), (3) combined T1w- and AICBV-predicted ages (TA-model), and (4) combined T1w- and AICBV-predicted ages with sex as an additional covariate (TAS-model) as shown in Table 1. Our models achieved strong performance metrics across T1w MRI, AICBV, and combined modalities along with the sex of the patient.

In Figure 3, scatter and residual plots are shown to demonstrate the goodness of fit for each model on the test data. The T-model yielded a mean absolute error (MAE) of 4.10 years and R^2 of 0.936. For AICBV alone, the A-model achieved MAE of 4.49 years and R^2 of 0.927. The combined TA-model, integrating both modalities as features of a linear regression model, achieved an MAE of 3.96 and R^2 of 0.943, surpassing traditional BrainAGE models based solely on T1w MRI. Adding sex as a feature in the TAS-model marginally improved performance, reducing the MAE to 3.95 and keeping the same and R^2 of 0.943. Table 1 contains the full results of each model created from the T1w-predicted age, AICBV-predicted age, and sex features with MAE, Mean Squared Error (MSE), and R2.

For each model, we performed ANOVA statistical tests to evaluate whether there were statistically significant differences in performance between the T-model and TA-model, A-model and TA-model, and TA-model and TAS-model. Comparisons between the T-model and TA-model, as well as between the A-model and TA-model, yielded highly significant p-values ($\alpha < 0.05$). These results highlight the substantial improvement achieved by incorporating both T1w MRI and AICBV data in the BrainAGE estimation task. When comparing the TA-model and TAS-model, the p-value was higher at 0.02, but still statistically significant. This finding demonstrates that including sex as an additional feature further enhances the model’s predictive performance. These results are also in Table 1.

3.2 Performance by Age Group

Age Group	T-model	A-model	TA-model	TAG-model
15-20	2.10	4.41	2.94	2.91
20-25	3.14	3.93	3.40	3.41
25-30	3.94	5.31	4.59	4.56
30-35	4.97	4.94	4.71	4.70
35-40	3.58	3.80	3.08	3.09
40-45	4.20	3.47	3.65	3.65
45-50	3.13	3.18	2.79	2.77
50-55	4.94	4.79	4.36	4.36
55-60	3.68	6.04	4.37	4.36
60-65	4.85	5.68	5.09	5.06
65-70	4.75	5.10	3.78	3.79
70-75	5.43	4.36	4.84	4.82
75-80	4.02	5.23	4.44	4.44
80-85	3.17	4.81	3.30	3.29
85-90	4.27	3.68	3.77	3.76
90-95	4.25	1.70	2.90	2.94

Table 2: Mean Absolute Error (MAE) Performance of Each Model for Each 5-Year Age Interval on the Test Data.

To further contextualize our findings, we visualized the MAE of each model across 5-year age groups within the test set in Table 2. As anticipated, the T-model and A-model generally exhibited higher MAE compared to the TA-model and TAS-model across most age groups. However, notable outliers emerged. In younger age groups, particularly between 15 and 30 years, the T-model demonstrated a lower MAE than its counterparts. This observation suggests that anatomical information from T1w MRI is more critical for accurately predicting age in younger individuals. Conversely, in older age groups, specifically between 85 and 95 years, the A-model consistently outperformed the others, with particularly pronounced accuracy in the 90 to 95 age group. This trend underscores the importance of incorporating functional information, such as AICBV, for accurately estimating age in older individuals.

3.3 Performance by Study

Project	T-model	A-model	TA-model	TAG-model
ADNI	3.55	3.88	3.34	3.33
AIBL	4.91	4.71	4.55	4.54
BGSP	2.76	3.34	3.05	3.04
CoRR	5.02	3.89	4.51	4.48
DLBS	4.87	5.70	4.91	4.95
IXI	4.28	5.21	4.19	4.17
NIFD	4.04	4.59	3.89	3.87
OAS1	4.84	4.90	4.83	4.80
OAS2	3.46	4.98	3.80	3.79
PPMI	4.39	3.72	3.97	3.94
SALD	4.38	4.86	4.04	4.04
SLIM	3.66	4.86	4.02	4.05
SchizConnect	3.69	4.19	3.49	3.48

Table 3: Mean Absolute Error (MAE) Performance of Each Model for Each Project on the Test Data.

To ensure the generalizability of our results across diverse patient populations, we calculated the MAE for each model across individual projects within the test set in Table 3. Overall, the models demonstrated consistent performance across projects, with only a few notable outliers. For example, the BGSP project exhibited a significantly lower MAE compared to most other projects. This likely reflects the age distribution of BGSP, which is skewed toward younger subjects—a demographic for which our model has already been shown to perform well. Conversely, the model underperformed on the dlbs study. While further investigation is required to fully understand this phenomenon, it is likely attributable to the study’s age distribution, which is skewed toward groups, such as individuals aged 55 to 65 years, where our model does not perform as effectively.

3.4 Gradient Maps for T1w and AICBV Inputs

To further support clinical applicability, we implemented a Grad-CAM visualization pipeline to identify the regions of input data—derived from either T1w MRI or AICBV—that had the greatest impact on the model’s predictions. This explainability mechanism is a vital step toward fostering trust and interpretability in clinical applications of the model. Specifically, we extracted the top 20% of gradient values from the final convolutional layer of the last block in each encoder and averaged them across the axial, coronal, and sagittal views. The slice that is used is determined by the maximum overall area of gradients on each individual slice to show where the model focuses most in the 3D volume input. For visualization, these gradient maps were overlaid on an average T1w scan for each 10-year age group, providing a clear representation of the regions most influential in the model’s decision-making process.

Figure 4 displays Grad-CAM visualizations for both the T1w and AICBV inputs respectively, revealing intriguing patterns in the model’s encoders. Notably, the T1w and AICBV encoders appear to focus on mutually exclusive regions when processing their respective input data. Specifically, the AICBV encoder frequently focuses on dense regions of blood within the central or lower portions of the brain. In contrast, the T1w encoder largely ignores these regions, instead prioritizing surrounding white matter structures. This distinct focus underscores the complementary nature of the two modalities, with AICBV capturing functional features that purely anatomical information from T1w MRI cannot provide, thereby enhancing the model’s predictive performance.

Another interesting pattern observed in the analysis is the shift in model focus across age groups, as revealed by the Grad-CAM visualizations. For the T1w encoder, there is a notable transition in the regions utilized for brain age prediction across the lifespan. In younger age groups, the model predominantly focuses on the medial prefrontal cortex, a region central to cognitive and emotional processes. However, in older age groups, this focus shifts bilaterally to the inferior frontal cortex (IFC). The IFC, particularly the inferior frontal gyrus (IFG), is a region known to exhibit significant age-related structural vulnerability, as evidenced by pronounced volume reductions over time [13]. The transition of the T1w encoder’s focus from the medial prefrontal cortex in younger individuals to the IFC in older adults underscores the interplay between regions involved in higher-order cognitive processes and those more vulnerable to structural decline. The IFC’s susceptibility to age-related atrophy and volume loss not only serves as a biomarker of aging but may also reflect broader changes in functional connectivity and neural efficiency that accompany aging [5]. These changes reflect the region’s susceptibility to atrophic processes with aging, aligning with findings in prior research.

For AICBV-based predictions, a similar age-related shift in focus is observed. In younger populations, the medial prefrontal cortex remains the primary region contributing to brain age estimation. However, as the population ages, the focus transitions to the medial temporal lobe, particularly the dentate gyrus. The dentate gyrus, a critical component of the hippocampal formation, demonstrates the most significant age-related functional changes in terms of CBV [5]. The AICBV-based predictions underscore the distinct functional markers of aging, particularly the transition from medial prefrontal cortex activity to the medial temporal lobe, with a specific focus on the dentate gyrus. The prominence of the dentate gyrus in older populations highlights the critical role of cerebral blood flow and neurovascular health in maintaining cognitive function. The pronounced decline in CBV within the dentate gyrus aligns with known reductions in neurogenesis and memory capacity, offering a physiological explanation for its relevance in brain age estimation [16].

4 Discussion

4.1 Performance Improvement with AICBV

Our approach, which integrates predictions from models trained on T1w MRI and AICBV, achieved a lower mean absolute error (MAE) than the similar model proposed by Feng et al. [6]. Their model, which utilized a similar architecture and was trained on the same large and heterogeneous dataset, relied solely on T1w MRI as input. This improved performance underscores not only enhanced predictive accuracy but also the successful incorporation of functional information into BrainAGE estimation—a longstanding objective in the field. AICBV provides an additional independent covariate that a T1w-trained model alone could not replicate due to a lack of prior knowledge of the importance of functional information. By leveraging the DeepC algorithm to generate functional information without requiring additional data collection, our study contributes a novel source of function information to BrainAGE modeling.

4.2 Regional Vulnerability and Sex Difference in Brain Aging

In our linear regression analyses, we systematically evaluated the inclusion and exclusion of specific feature sets: (1) T1w-predicted age only (T-model), (2) AICBV-predicted age only (A-model), (3) combined T1w- and AICBV-predicted ages (TA-model), and (4) combined T1w- and AICBV-predicted ages with sex as an additional covariate (TAS-model). Among these, the TAS-model achieved the lowest MAE of 3.95. Notably, the coefficient for sex in this model was -0.168 , with a p-value of 0.02, below the standard significance threshold of $\alpha = 0.05$. Given that sex was coded as 0 for female and 1 for male, this negative coefficient suggests that the model adjusts male age predictions downward, indicating that male brains are perceived as appearing older than female brains. This result aligns with established clinical evidence of sex-related differences in brain aging, further validating the model’s anatomical and physiological insights [1, 3].

4.3 Clinical Implications

The integration of AICBV with structural T1w MRI scans offers significant potential for advancing clinical brain aging assessments. Our model demonstrates that combining functional and structural imaging modalities leads to more accurate predictions of brain age, especially in older populations. This could be particularly valuable in clinical settings for the early detection of neurodegenerative diseases such as Alzheimer’s disease, where subtle functional changes precede visible structural atrophy [23]. Furthermore, the ability to get this functional information from non-invasive MRI scans without the need for further risky measures provides a safer alternative to accessing this valuable context. By providing a more comprehensive view of brain health, this approach has the potential to enhance clinical decision-making, offering a valuable tool for both research and routine clinical practice.

BrainAGE has served as a valuable neuroimaging biomarker in clinical practice, offering insights into individual brain aging trajectories [19, 21]. BrainAGE, by estimating the difference between predicted brain age and chronological age, serves as a potential biomarker for detecting neuroanatomical changes that may precede clinical symptoms of neurodegenerative diseases [4]. However, its application faces limitations when only considering structural information in its prediction. Our integrated structural and functional approach captures both the architectural integrity and subtle vascular changes, potentially offering a more sensitive indicator of incipient neurodegenerative trajectories. This integrated biomarker could be invaluable for monitoring disease progression and evaluating the efficacy of novel interventions, guiding clinicians to intervene earlier in the disease course. Our method capitalizes on routine MRI scans and delivers functional-like insights without additional procedures, broadening its potential impact in both preclinical research and everyday patient care.

Additionally, while BrainAGE provides a valuable snapshot of an individual’s current brain health, it does not fully capture the dynamic progression of underlying pathophysiological changes as they unfold over time [7]. Understanding the trajectory of a patient’s aging process—rather than relying on a single timepoint—can be crucial for identifying subtle, cumulative shifts that may signal the early onset or accelerated progression of neurological diseases [14, 22]. By expanding this biomarker to account for longitudinal data, clinicians could tailor its application to individual patients, allowing the model to detect deviations in both structural

integrity and functional vascular changes relative to an expected aging paradigm. This personalized, time-sensitive approach has the potential to reveal emerging disease states at an earlier stage, guiding timely intervention and more precise patient management.

5 Conclusion

In this study, we demonstrated that integrating anatomical (T1w MRI) and functional (AICBV) data improves the accuracy of BrainAGE prediction, showcasing the synergistic value of structural and functional data. Additionally, our findings align with clinical understandings of brain aging, further validating the utility of our approach.

Future work will explore novel deep learning architectures, including transformer-based models and cross-encoder designs, to more effectively integrate anatomical and functional data and further enhance model performance. These approaches also have the potential to enhance local explainability, providing anatomically grounded insights into predictions. Emerging advances in unsupervised and latent space learning can further enhance the clinical applicability of these models. Recent works have leveraged unsupervised deep learning to extract latent vulnerability maps and saliency regions from neuroimaging data [5, 23]. Adapting these latent space approaches to BrainAGE modeling could identify hidden disease signatures and vulnerability pathways without requiring extensive labeled training data. This additional layer of interpretability would not only improve the precision and reliability of brain age predictions, but would also guide clinicians toward more targeted interventions, personalized monitoring regimens, and a deeper understanding of the complex interplay between structural and functional changes in the aging and diseased brain. In this way, the combination of multimodal imaging, robust modeling strategies, and unsupervised learning techniques holds promise for elevating BrainAGE from a research tool into a clinically actionable biomarker.

Moreover, the development of more advanced XAI methods, such as utilizing large language models to generate multimodal, free-text explanations, could make these models more accessible to clinicians, seamlessly integrating explainability into their workflows. Finally, conducting translational studies will be crucial to validate these models in real-world clinical settings and assess their impact on patient care outcomes. By addressing these avenues, we aim to bridge the gap between cutting-edge machine learning research and its practical application in healthcare.

6 Figures

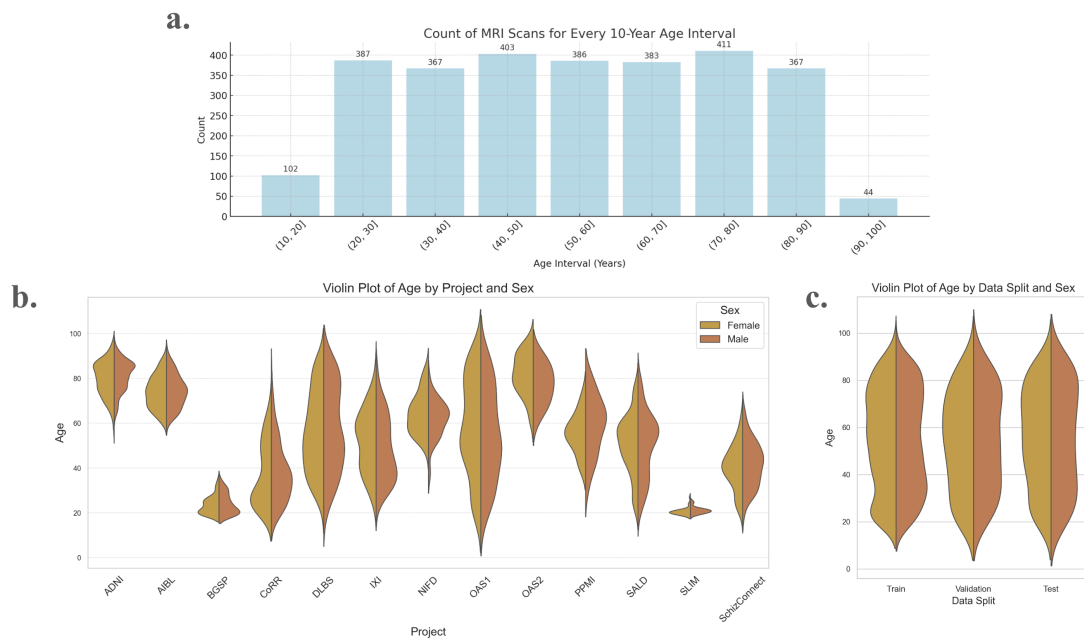


Fig. 1: (a) The count of subject age per 10-year interval within the dataset. (b) The distribution of age and sex for each study in the dataset that the MRI scans were sourced from. (c) Distribution of ages in each data split used to train and test the model including the training, validation, and test set.

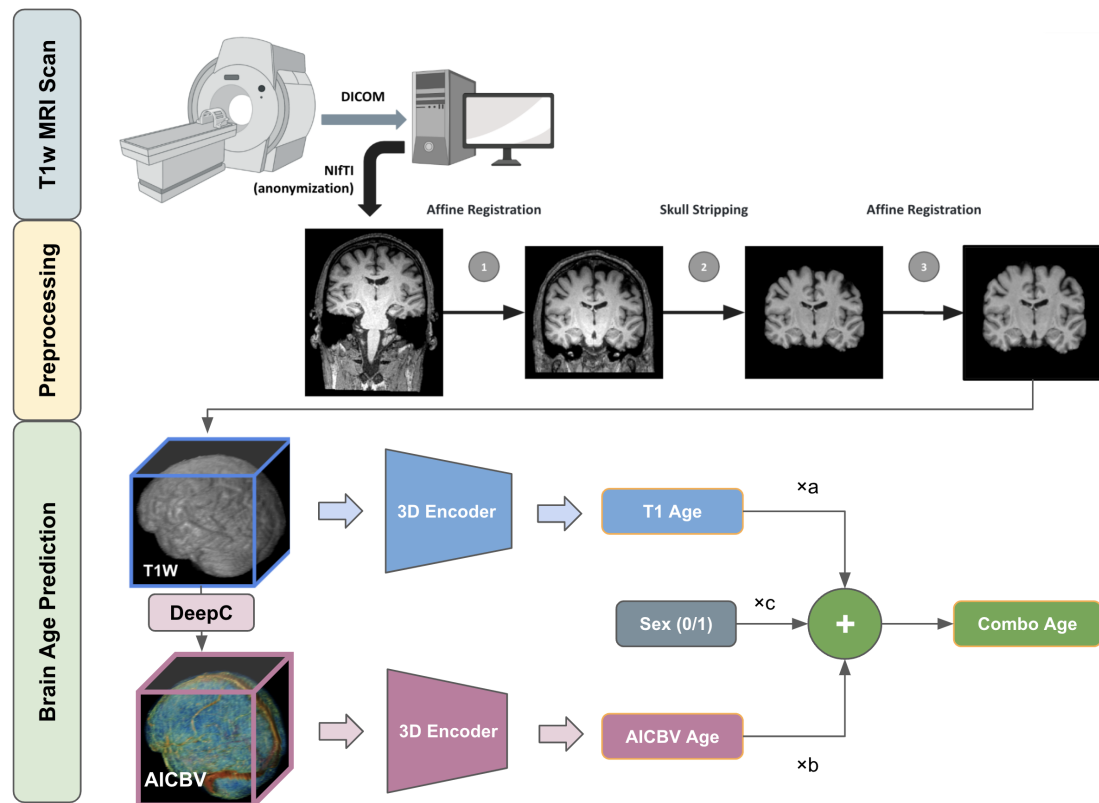


Fig. 2: General pipeline for estimating brain age from T1w MRI and AICBV with deep learning models and a linear regression model to combine their predictions.

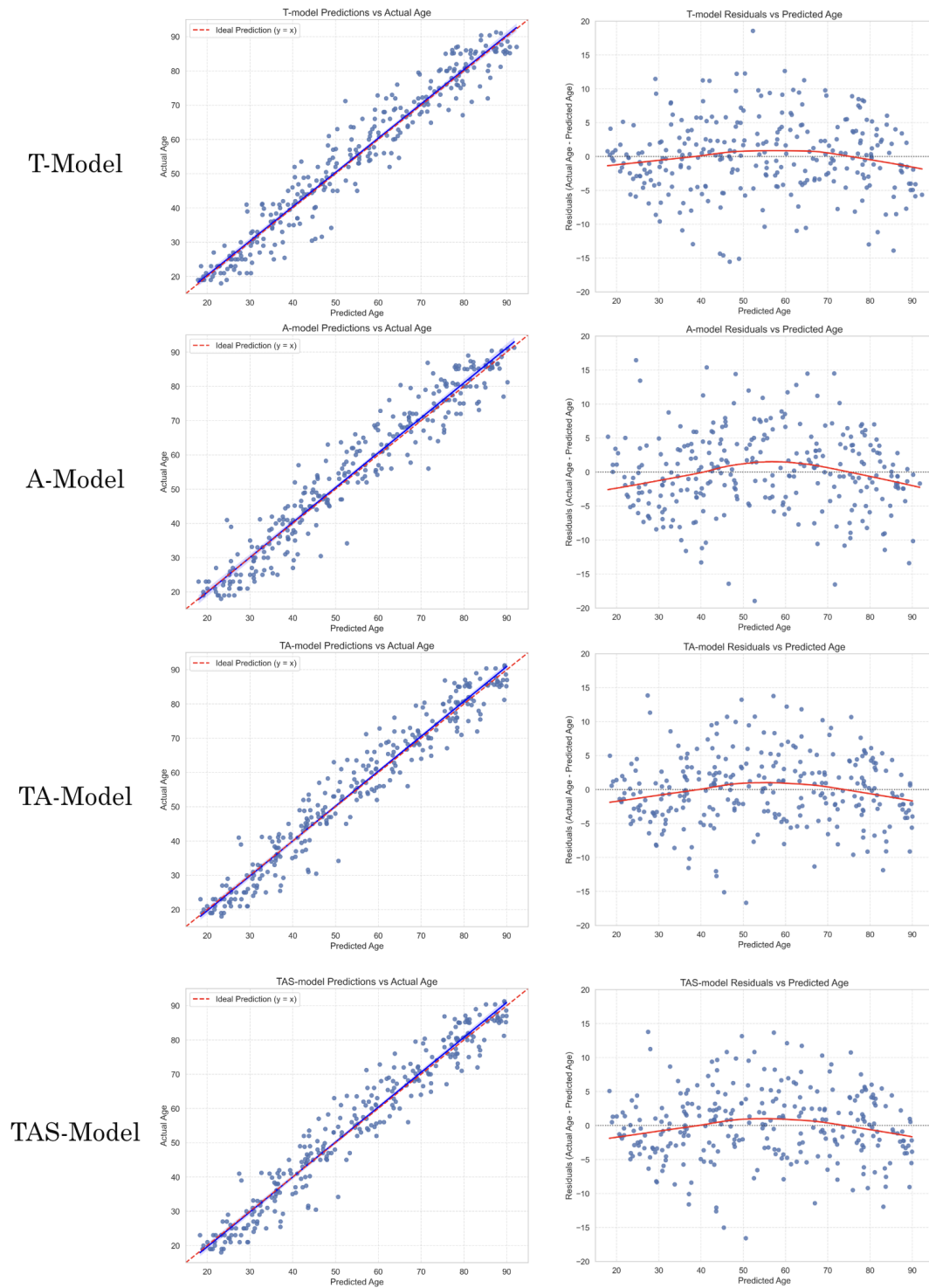


Fig. 3: Scatter and residual plots for each model on the test data set.

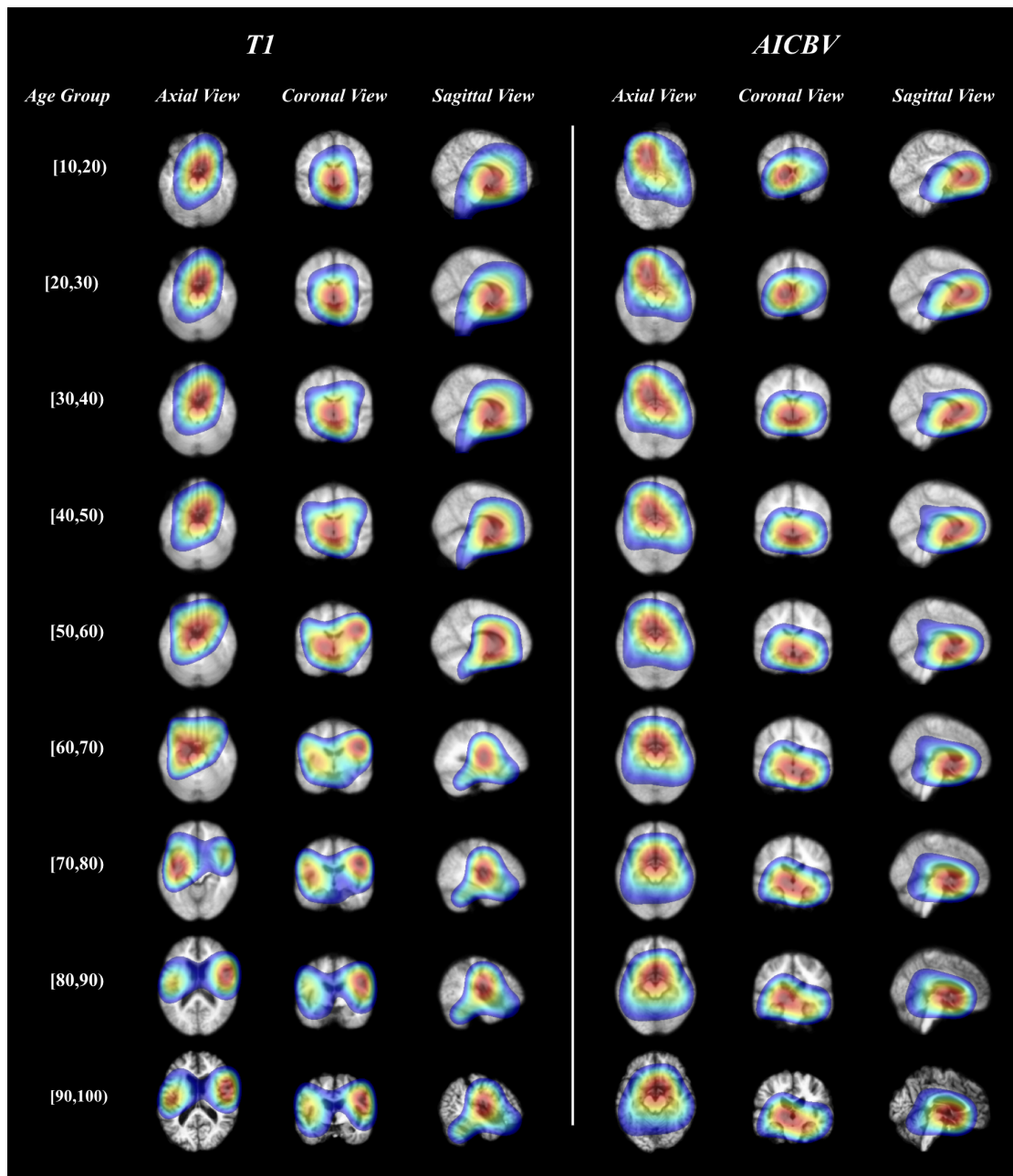


Fig. 4: Average top 20% gradient values from T1w and AICBV encoder are overlaid on average T1w MRI scans for each 10-year age group.

References

- [1] Armstrong, N.M., An, Y., Beason-Held, L., Doshi, J., Erus, G., Ferrucci, L., Davatzikos, C., Resnick, S.M.: Sex differences in brain aging and predictors of neurodegeneration in cognitively healthy older adults. *Neurobiology of Aging* **81**, 146–156 (Sep 2019). <https://doi.org/10.1016/j.neurobiolaging.2019.05.020>, <https://www.sciencedirect.com/science/article/pii/S0197458019301769>
- [2] Barbier, E.L., Lamalle, L., Décorps, M.: Methodology of brain perfusion imaging. *Journal of Magnetic Resonance Imaging* **13**(4), 496–520 (2001). <https://doi.org/10.1002/jmri.1073>, <https://onlinelibrary.wiley.com/doi/abs/10.1002/jmri.1073>, [_eprint: https://onlinelibrary.wiley.com/doi/pdf/10.1002/jmri.1073](https://onlinelibrary.wiley.com/doi/pdf/10.1002/jmri.1073)
- [3] Coffey, C.E., Lucke, J.F., Saxton, J.A., Ratcliff, G., Unitas, L.J., Billig, B., Bryan, R.N.: Sex Differences in Brain Aging: A Quantitative Magnetic Resonance Imaging Study. *Archives of Neurology* **55**(2), 169–179 (Feb 1998). <https://doi.org/10.1001/archneur.55.2.169>, <https://doi.org/10.1001/archneur.55.2.169>
- [4] Cumplido-Mayoral, I., García-Prat, M., Operto, G., Falcon, C., Shekari, M., Cacciaglia, R., Milà-Alomà, M., Lorenzini, L., Ingala, S., Meije Wink, A., Mutsaerts, H.J., Minguillón, C., Fauria, K., Molinuevo, J.L., Haller, S., Chetelat, G., Waldman, A., Schwarz, A.J., Barkhof, F., Suridjan, I., Kollmorgen, G., Bayfield, A., Zetterberg, H., Blennow, K., Suárez-Calvet, M., Vilaplana, V., Gispert, J.D., ALFA study, EPAD study, ADNI study, OASIS study: Biological brain age prediction using machine learning on structural neuroimaging data: Multi-cohort validation against biomarkers of Alzheimer’s disease and neurodegeneration stratified by sex. *eLife* **12**, e81067 (Apr 2023). <https://doi.org/10.7554/eLife.81067>, <https://doi.org/10.7554/eLife.81067>, publisher: eLife Sciences Publications, Ltd
- [5] Feng, X., Guo, J., Sigmon, H.C., Sloan, R.P., Brickman, A.M., Provenzano, F.A., Small, S.A., Initiative, f.t.A.D.N.: Brain regions vulnerable and resistant to aging without Alzheimer’s disease. *PLoS One* **15**(7), e0234255 (Jul 2020). <https://doi.org/10.1371/journal.pone.0234255>, <https://www.proquest.com/docview/2428410132/abstract/C5C6A2F3AB5547BEPQ/1>, num Pages: e0234255 Place: San Francisco, United States Publisher: Public Library of Science Section: Research Article
- [6] Feng, X., Lipton, Z.C., Yang, J., Small, S.A., Provenzano, F.A.: Estimating brain age based on a uniform healthy population with deep learning and structural magnetic resonance imaging. *Neurobiology of Aging* **91**, 15–25 (Jul 2020). <https://doi.org/10.1016/j.neurobiolaging.2020.02.009>, <https://www.sciencedirect.com/science/article/pii/S0197458020300361>
- [7] Franke, K., Gaser, C.: Ten Years of BrainAGE as a Neuroimaging Biomarker of Brain Aging: What Insights Have We Gained? *Front. Neurol.* **10** (Aug 2019). <https://doi.org/10.3389/fneur.2019.00789>, <https://www.frontiersin.org/journals/neurology/articles/10.3389/fneur.2019.00789/full>, publisher: Frontiers
- [8] Gallach, M., Lette, M.M., Abdel-Wahab, M., Giammarile, F., Pellet, O., Paez, D.: Addressing Global Inequities in Positron Emission Tomography-Computed Tomography (PET-CT) for Cancer Management: A Statistical Model to Guide Strategic Planning. *Med Sci Monit* **26**, 0–0 (Aug 2020). <https://doi.org/10.12659/MSM.926544>, <https://www.medscimonit.com/abstract/full/idArt/926544>, publisher: International Scientific Information, Inc.
- [9] Glover, G.H.: Overview of Functional Magnetic Resonance Imaging. *Neurosurg Clin N Am* **22**(2), 133–139 (Apr 2011). <https://doi.org/10.1016/j.nec.2010.11.001>, <https://www.ncbi.nlm.nih.gov/pmc/articles/PMC3073717/>
- [10] Ibrahim, M.A., Hazhirkarzar, B., Dublin, A.B.: Gadolinium Magnetic Resonance Imaging. In: *StatPearls*. StatPearls Publishing, Treasure Island (FL) (2024), <http://www.ncbi.nlm.nih.gov/books/NBK482487/>
- [11] Lee, J., Kim, H.J.: Normal Aging Induces Changes in the Brain and Neurodegeneration Progress: Review of the Structural, Biochemical, Metabolic, Cellular, and Molecular Changes. *Front. Aging Neurosci.* **14** (Jun 2022). <https://doi.org/10.3389/fnagi.2022.931536>, <https://www.frontiersin.org/journals/aging-neuroscience/articles/10.3389/fnagi.2022.931536/full>, publisher: Frontiers
- [12] Liu, C., Zhu, N., Sun, H., Zhang, J., Feng, X., Gjerswold-Selleck, S., Sikka, D., Zhu, X., Liu, X., Nuriel, T., Wei, H.J., Wu, C.C., Vaughan, J.T., Laine, A.F., Provenzano, F.A.,

- Small, S.A., Guo, J.: Deep learning of MRI contrast enhancement for mapping cerebral blood volume from single-modal non-contrast scans of aging and Alzheimer’s disease brains. *Front. Aging Neurosci.* **14** (Aug 2022). <https://doi.org/10.3389/fnagi.2022.923673>, <https://www.frontiersin.org/journals/aging-neuroscience/articles/10.3389/fnagi.2022.923673/full>, publisher: Frontiers
- [13] McGinnis, S.M., Brickhouse, M., Pascual, B., Dickerson, B.C.: Age-Related Changes in the Thickness of Cortical Zones in Humans. *Brain Topogr* **24**(3), 279–291 (Oct 2011). <https://doi.org/10.1007/s10548-011-0198-6>, <https://doi.org/10.1007/s10548-011-0198-6>
- [14] Nguyen, H., Clément, M., Mansencal, B., Coupé, P.: Brain structure ages—A new biomarker for multi-disease classification. *Hum Brain Mapp* **45**(1), e26558 (Jan 2024). <https://doi.org/10.1002/hbm.26558>, <https://www.ncbi.nlm.nih.gov/pmc/articles/PMC10785199/>
- [15] Ohn, S.H.: Cerebral Blood Volume Magnetic Resonance Imaging. *Brain & Neurorehabilitation* **11**(2) (Jul 2018). <https://doi.org/10.12786/bn.2018.11.e18>, <https://doi.org/10.12786/bn.2018.11.e18>
- [16] Pereira, A.C., Huddleston, D.E., Brickman, A.M., Sosunov, A.A., Hen, R., McKhann, G.M., Sloan, R., Gage, F.H., Brown, T.R., Small, S.A.: An in vivo correlate of exercise-induced neurogenesis in the adult dentate gyrus. *Proc Natl Acad Sci U S A* **104**(13), 5638–5643 (Mar 2007). <https://doi.org/10.1073/pnas.0611721104>
- [17] Schulz, M., Mayer, C., Schlemm, E., Frey, B.M., Malherbe, C., Petersen, M., Gallinat, J., Kühn, S., Fiehler, J., Hanning, U., Twerenbold, R., Gerloff, C., Cheng, B., Thomalla, G.: Association of Age and Structural Brain Changes With Functional Connectivity and Executive Function in a Middle-Aged to Older Population-Based Cohort. *Front. Aging Neurosci.* **14** (Feb 2022). <https://doi.org/10.3389/fnagi.2022.782738>, <https://www.frontiersin.org/journals/aging-neuroscience/articles/10.3389/fnagi.2022.782738/full>, publisher: Frontiers
- [18] Small, S.A., Schobel, S.A., Buxton, R.B., Witter, M.P., Barnes, C.A.: A pathophysiological framework of hippocampal dysfunction in ageing and disease. *Nat Rev Neurosci* **12**(10), 585–601 (Oct 2011). <https://doi.org/10.1038/nrn3085>, <https://www.nature.com/articles/nrn3085>, publisher: Nature Publishing Group
- [19] Sone, D., Beheshti, I.: Neuroimaging-Based Brain Age Estimation: A Promising Personalized Biomarker in Neuropsychiatry. *Journal of Personalized Medicine* **12**(11), 1850 (Nov 2022). <https://doi.org/10.3390/jpm12111850>, <https://www.mdpi.com/2075-4426/12/11/1850>, number: 11 Publisher: Multidisciplinary Digital Publishing Institute
- [20] Varallyay, C.G., Nesbit, E., Fu, R., Gahramanov, S., Moloney, B., Earl, E., Muldoon, L.L., Li, X., Rooney, W.D., Neuwelt, E.A.: High-resolution steady-state cerebral blood volume maps in patients with central nervous system neoplasms using ferumoxytol, a superparamagnetic iron oxide nanoparticle. *J Cereb Blood Flow Metab* **33**(5), 780–786 (May 2013). <https://doi.org/10.1038/jcbfm.2013.36>, <https://www.ncbi.nlm.nih.gov/pmc/articles/PMC3653563/>
- [21] Wittens, M.M., Denissen, S., Sima, D.M., Fransen, E., Niemantsverdriet, E., Bastin, C., Benoit, F., Bergmans, B., Bier, J.C., de Deyn, P.P., Deryck, O., Hanseeuw, B., Ivanoiu, A., Picard, G., Ribbens, A., Salmon, E., Segers, K., Sieben, A., Struyfs, H., Thiery, E., Tournoy, J., van Binst, A.M., Versijpt, J., Smeets, D., Bjerke, M., Nagels, G., Engelborghs, S.: Brain age as a biomarker for pathological versus healthy ageing – a REMEMBER study. *Alz Res Therapy* **16**(1), 128 (Jun 2024). <https://doi.org/10.1186/s13195-024-01491-y>, <https://doi.org/10.1186/s13195-024-01491-y>
- [22] Zhu, J.D., Wu, Y.F., Tsai, S.J., Lin, C.P., Yang, A.C.: Investigating brain aging trajectory deviations in different brain regions of individuals with schizophrenia using multimodal magnetic resonance imaging and brain-age prediction: a multicenter study. *Transl Psychiatry* **13**, 82 (Mar 2023). <https://doi.org/10.1038/s41398-023-02379-5>, <https://www.ncbi.nlm.nih.gov/pmc/articles/PMC9992684/>
- [23] Zhu, N., Liu, C., Feng, X., Sikka, D., Gjerswold-Selleck, S., Small, S.A., Guo, J.: Deep Learning Identifies Neuroimaging Signatures of Alzheimer’s Disease Using Structural and Synthesized Functional MRI Data. In: 2021 IEEE 18th International Symposium on Biomedical Imaging (ISBI). pp. 216–220 (Apr 2021). <https://doi.org/10.1109/ISBI48211.2021.9433808>, <http://arxiv.org/abs/2104.04672>, arXiv:2104.04672 [cs, q-bio]